Spacecraft materials degradation under space-simulated low Earth orbit (LEO) environment

Elena A. Plis*
Georgia Tech Research Institute (GTRI), Atlanta, GA, 30318, USA; Assurance Technology Corporation, Carlisle, MA, 01741, USA

Miles T. Bengtson†
National Research Council Research Associateship Program, 3550 Aberdeen Ave., Kirtland AFB, New Mexico 87117, USA

Daniel P. Engelhart‡
University of New Mexico, Albuquerque, NM, 87131, USA

Gregory P. Badura§
Georgia Tech Research Institute (GTRI), 925 Dalney St NW, Atlanta, GA 30318

Heather M. Cowardin¶
NASA Johnson Space Center, Orbital Debris Program Office, 2101 NASA Pkwy., Houston, TX 77058, USA

Jacqueline A. Reyes‖
University of Texas at El Paso, 500 W. University Ave., El Paso, TX, 79968, USA

Ryan C. Hoffmann, Alexey Sokolovskiy, Dale C. Ferguson**
Air Force Research Laboratory, Space Vehicles Directorate, USA, Kirtland AFB, Albuquerque, NM, 87117, USA

Jainisha R. Shah and Sydney Collman, ††
Assurance Technology Corporation, Carlisle, MA, 01741, USA

Timothy R. Scott‡‡
DuPont de Nemours, Inc, Durham, NC 27703, USA

External spacecraft materials play an important role in satellite protection from the harsh space environment. Research has shown that the physical, chemical, and optical properties of matter change continuously as a result of exposure to solar radiation and aggressive chemical species produced in Earth's upper atmosphere. Thorough knowledge of the material properties evolution throughout a planned mission lifetime helps to improve the reliability of spacecraft. Moreover, the establishment of correlation factors between true space exposure and accelerated space weather experiments at ground facilities enables accurate prediction of on-orbit material performance based on laboratory-based testing. The presented work aims to evaluate the

*Senior Research Engineer, Georgia Tech Research Institute (GTRI), 925 Dalney St NW, Atlanta, GA 30318; Assurance Technology Corporation, Carlisle, MA, 01741, USA

†Postdoctoral Fellow, National Research Council Research Associateship Program, 3550 Aberdeen Ave., Kirtland AFB, New Mexico 87117, USA

‡Research Professor, Department of Chemistry and Chemical Biology, University of New Mexico, 300 Terrace St NE, Albuquerque, NM, 87131.

§Research Scientist, Georgia Tech Research Institute (GTRI), 925 Dalney St NW, Atlanta, GA 30318.

¶Laboratory and In Situ Lead Orbital Debris Business Unit Manager, NASA Johnson Space Center, Orbital Debris Program Office, 2101 NASA Pkwy., Houston, TX 77058, USA

‖University of Texas at El Paso, 500 W. University Ave., El Paso, TX, 79968, USA

**Air Force Research Laboratory, Space Vehicles Directorate, USA, Kirtland AFB, Albuquerque, NM, 87117, USA

††Assurance Technology Corporation, Carlisle, MA, 01741, USA

‡‡Business Development Leader, Aerospace & Defense, DuPont de Nemours, Inc, Durham, NC 27703.

radiation effects of low Earth orbit (LEO) environment, namely, exposure to the high-energy electrons, atomic oxygen (AO), and vacuum ultraviolet (VUV), of several modern spacecraft materials. The studied materials represent the "flight duplicates" of samples that are launched as a part of the 16th Materials International Space Station Experiment Flight Facility (MISSE-FF) mission in 2022.

I. Introduction

During the mission, surface spacecraft materials are exposed to a number of environmental factors, including various types of ionizing radiation, electrons and protons of various energies, oxygen ions and atoms, micrometeoroids, vacuum, and large temperature fluctuations [1–6]. This exposure affects the physical and chemical properties of materials, thus degrading the functionality of the elements comprised from them and shortening the spacecraft lifetime. Therefore, a thorough knowledge of the evolution of material properties throughout a planned mission lifetime is of primary importance when designing long-term space missions. Further, as the requirements for new space missions become more stringent and extensive, novel lightweight materials needs to be developed with improved long-term radiation shielding and mechanical properties for use in internal and external spacecraft systems. Newly developed materials must be thoroughly vetted before implementation. Characterization of heritage materials in the space environment is also necessary for identification and tracking of orbital debris, a crucial first step toward debris remediation [7, 8].

Ground-based simulation of the space environment is experimentally challenging because the space environment varies wildly depending on orbit, solar conditions, and many other factors [9]. Simultaneous exposure of materials to the charge particles, VUV, and/or temperature may be hindered by different acceleration factors for particles and VUV flux, leading to significantly longer VUV irradiation times [10]. Oppositely, once a sequential exposure approach is utilized, materials are exposed to particles (protons, electrons) and VUV, in successive steps. Thus, degradation induced by each environmental component may be monitored separately.

Further, common spacecraft materials such as polyimides (PIs, Kapton®family) or polyethyleneterephthalates (PETs, Mylar®), are highly stable in their pristine state but become reactive once damaged with radiation [11, 12]. Unlike irradiation-induced material degradation which typically takes place under high vacuum conditions, the subsequent material handling and characterization is often performed in an uncontrolled laboratory atmosphere. As a result, chemical reaction of atmospheric gases with the highly reactive radiation-modified materials leads to healing, or recovery, of the damaged material properties, in particular, reflectivity. Since direct correlation of the reflectivity of dielectric materials with their physical and electrical properties has been previously demonstrated, then the characterization of the irradiated materials ex-situ makes the effect of actual space weather damage unrepresentative.

Development of microstructural, chemical structure, charge transport, and optical characterization capabilities integrated with the irradiation facility could elucidate experimentally the physics and chemistry of radiation-induced material properties. The importance of such integrated toolbox development was realized a while ago [13]; however, integration of material characterization techniques with the aging facility still represents a scientific and technical challenge. Thus, to ensure that material properties of space-weather exposed samples are not affected by the atmospheric exposure, handling and characterization protocols of the irradiated air-sensitive materials must be scrutinized and carefully controlled.

Geographically, collaborators working on preparation and characterization of materials exposed to the space-simulated conditions may be separated by hundreds of miles. As shown in Figure 1, the electron and VUV space-simulated exposure of materials for this study is performed at the Spacecraft Charging and Instrument Calibration Laboratory (SCICL) at the Kirtland AFRL (Albuquerque, NM) [14], whereas AO exposure was outsourced to Physical Sciences Inc [15]. Characterization of the space weather effects on material properties of spacecraft materials was performed in-situ at the SCICL, and ex-situ at the GTRI (Atlanta, GA) and the NASA Johnson Space Center (Houston, TX). Thus, it needs to be ensured that all collaborators are receiving space-weather exposed samples that have minimally affected by their recovery in atmosphere prior characterization, and that all characterization procedures are performed with the minimized air exposure.

Finally, degradation of spacecraft materials induced by the space-simulated conditions as well as exposure techniques themselves are not validated by the real space or ground observations and, in addition, there is a need of improvement of predictive models describing the space-weather-induced material changes. The the Materials International Space Station Experiment Flight Facility (MISSE-FF) at International Space Station (ISS) is the perfect test bed to generate benchmark data with which to validate the efficacy of ground-based space weather simulation experiments [16, 17]. Insight into surface, chemical, and optical state of the materials prepared in the laboratory will help to fill the gaps

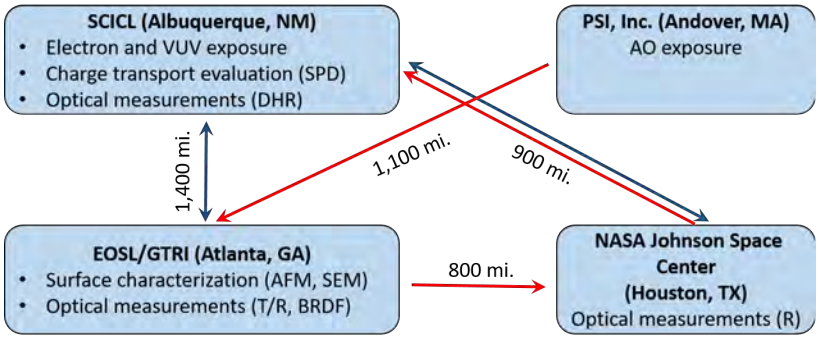

Fig. 1 Transfer logistics of materials exposed to the space-simulated environment between the partner organizations. Red lines correspond to the AO-exposed materials, and blue lines correspond to the materials irradiated with electrons and VUV particles.

between the materials state of resident space objects (RSOs) and the laboratory experiments.

In presented work, several spacecraft polymers were first thoroughly characterized in their pristine state to create a baseline for the ground- and space-based experiments. Next, alteration of optical, surface, and charge transport properties of the same materials were studied under space-simulated environment comprised by, separately, high-energy electron, AO, and VUV exposure. The same material selection is launched during the MISSE-16 mission; the preliminary space experiment data as well as their comparison with the results of ground experiments will also be discussed during the presentation.

II. Experimental Details

A. Materials

MISSE flight sample collection comprises several different classes of polymers a shown in figure 2. This work focuses on several materials from the Kapton®family (Kapton®TH, Kapton®CR, and Kapton®HN), carbon fiber reinforced polymer (CFRP), and glass fiber reinforced polymer (GFRP).

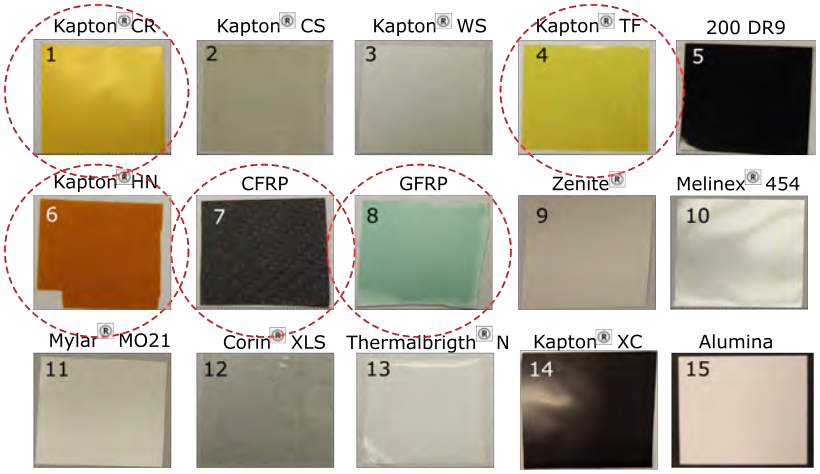

Fig. 2 MISSE-FF sample collection. The present study focuses on materials denoted with red dashed circles. Trade names and trademarks are used in this report for identification only. Their usage does not constitute an official endorsement, either expressed or implied, by the National Aeronautics and Space Administration.

Kapton®HN has been used for more than 50 years to protect nearly every satellite, spacecraft, and astronaut since Apollo 11. This well-studied film is utilized as a reference material for our ground and space experiments.Kapton®CR is a corona-resistant material which may be potentially utilized for shielding of sensitive equipment on-board of a spacecraft.

Kapton®TF is thermoformable material; it's a possible candidate for small satellite parts manufacturing. CFRP and GFRP are two examples of modern materials used in the construction of present-day LEO satellites. Unfortunately, minimal tests have been conducted in laboratory settings to better characterize their optical properties and potential degradation in the LEO environment.

B. Material Handling

The operational procedure developed by the SCICL for handling of spacecraft materials sensitive to atmospheric exposure secures enough time for air-sensitive materials delivery [18]. The sealing procedure comprises vacuum sealing under Argon flush using double-layered plastic bags with humectant and two oxygen absorbers securely placed inside the first bag.

C. Irradiation procedure

High energy electron and VUV exposure were performed sequentially in the Jumbo space irradiation chamber at the SCICL [14]. Materials were bombarded with high energy (100 keV) electrons produced by a mono-energetic Kimball Physics EG8105-UD electron flood gun. In according to [19], mean annual electron flux (>100 keV, electrons, orbit averaged) experienced by the ISS is $\sim 10^{13}$ electrons/cm^2/second. The maximum electron fluence the materials under investigation were exposed to is 8.5 x 10^{13} electrons/cm^2, which corresponds to approximately ten years at 600-800 km (LEO) orbit, delivered during 5.5 hours. Details of the electron irradiation procedure are reported elsewhere [11]. The VUV illumination that MISSE-FF samples received on-board of the ISS can be expressed by the number of equivalent sun hours (ESH), which is equal to the UV part of the solar spectrum integrated over 1 hour [20]. The ISS orbits Earth every 90 minutes, and with the anticipated duration of MISSE-16 experiment of 6 months, samples were exposed to maximum of 2190 ESH, or 3.5 x 10^8 J/m^2.

AO exposure was performed using the FAST source at the Physical Sciences Inc. in according to ASTM-E2089-15. The effective peak atomic oxygen fluence during the exposure was 3.1 x 10^{20} O/cm^2 which corresponds to 6 weeks of LEO exposure. Details of AO-irradiation procedure may be found in [21].

D. Materials characterization

1. Surface properties

Surface morphology and roughness of studied materials was examined using Bruker Dimension ICON atomic force microscopy (AFM) allowing measurement of surface roughness up to 5 μm on areas as large as 200 μm x 200 μm. In addition, SEM measurements were performed on AO-irradiadted CFRP and GFRP materials.

2. Optical properties

The direct hemispherical reflectance (DHR) measurements of pristine and space-weather exposed films were performed prior and during the electron irradiation procedure in according to the optical data acquisition procedure reported elsewhere [22]. Transmission measurements of AO-exposed materials were perfomed with the Gary 5000 UV-Vis-NIR spectrometer.

The Hemispherical Conical Reflectance Factor (HCRF), the laboratory approximation of true Bidirectional Reflectance Distribution Function (BRDF) measurements, of pristine samples with fixed viewing angles (0°, 30°, 60°, -30°, and -60°) and variable illumination angles (0° - 70° degrees range, exact values of illumination angles are specified separately for each measurement), was evaluated in the principal plane of illumination. The samples were illuminated with a collimated 50 Watt tungsten halogen that approximated a blackbody source over the range of 350-2500 nm. An Analytical Spectral Devices Spectrometer was used to collect radiance measurements over this spectral range [23].

3. Charge transport properties

To assess the charge transport properties of pristine and irradiated materials the ASTM D-257 measurements of materials' resistivity were performed. In addition, the surface potential decay (SPD) method was utilized [24].

4. Mass loss

Mass loss of AO-exposed materials was measured with 10 microgram accuracy using the microgram balance. Prior weight measurements, all samples were stored in the vacuum chamber for 24 hours to remove water. They were then removed and weighed over time to monitor water absorption and allow for the dry mass to be calculated. Next, AO-erosion rate was estimated.

III. Results and Discussion

Table 1 summarizes the surface roughness of pristine, electron-irradiated, and AO-exposed samples accessed by AFM. VUV results will be discussed during the presentation. Average surface roughness (R_a) values are average of several 5μm x 5μm scans taken at different parts of the pristine and electron-irradiated samples. Note, that roughness of CFRP material was too large even in its pristine form to be measured reliably with the AFM technique. SEM measurements is the option of choice for the surface morphology characterization of this particular material. Representative 5μm x 5μm AFM scans of pristine, electron-irradiated, and AO-exposed material are shown in Figure 3.

The studied materials from the Kapton®family demonstrated different surface characteristics after electron exposure. Kapton®HN revealed significant reduction of RMS roughness, Kapton®CR did not change, and Kapton®TF showed increased surface roughening after electron bombardment. Exposure of polymer materials to AO at 8 km/s is sufficient to break the polymer bonds and induce oxidative decomposition, resulting in substantial erosion of polymer surfaces which manifests itself as the mass loss, thinning, and texture roughening. AO exposure clearly affected the surface roughness of the studied materials. All polymers from Kapton®family revealed a matter surface which is result of O-atom erosion leading to the microscopic roughness of these samples. AO-induced damage of GFRP, and CFRP materials manifested itself in an increased diffuse reflectance characteristics of AO-exposed surfaces.

Table 1 Surface roughness of pristine and electron-irradiated polymer samples

Material	Pristine (R_a, nm)	Electron-irradiated (R_a, nm)	AO-exposed (R_a, nm)
Kapton®HN	11.4	2.5	91.0
Kapton®CR	26.7	25.6	62.9
Kapton®TF	5.5	12.3	136.3
GFRP	12.2	4.6	218.0

SEM measurements of electron-irradiated, VUV, and most of the AO-exposed materials were not performed due to charging effects resulting in blurred SEM images. Solution for this issue includes coating of the damaged materials' surface with conductive metal, e.g., gold. Due to the nature of electron and VUV particles we did not expect to reveal a significant surface modifications of the electron-bombarded and VUV-exposed samples, which was confirmed by the visual inspection of irradiated materials as well as AFM data. Thus, SEM measurements were not intended for electron-irradiated materials. Oppositely, AO-exposed samples demonstrated a significant color change compared to pristine materials. Optical and SEM images confirmed the erosion of the AO-exposed samples. However, since AO-exposed MISSE materials set includes one coupon of every material, we decided to avoid their surface degradation with conductive coating. All AO-exposed sample were attempted for the SEM measurements; the corresponding SEM images of AO-exposed CFRP and GFRP materials are shown in Figures 4 and 4, respectively.

After AO-exposure, eroded areas were formed on the AO-exposed side of the CFRP sample. No such sites are featured on the surface of pristine CFRP material. SEM images of AO-exposed GFRP material reveal formation of erosion sites on the AO-treated surfaces as well. It's interesting to note that at lower magnification the eroded cites are not clearly visible whereas at higher magnification their presence is unquestionable.

Values of volume resistivities of pristine and electron-irradiated with maximum fluence materials measured by the ASTM and SPD methods are summarized in Figure 6. Charge transport properties of all irradiated materials were affected by the space-simulated irradiation in a similar manner; the overall decreased resistivity was demonstrated. The change of bulk resistivity of AO-exposed materials is shown in Figure 7. Results of SPD and ASTM measurements after VUV exposure will be discussed during the presentation.

Alike other PI films [19], the observed bulk resistivity decrease (i.e., conductivity increase) in electron-irradiated PI films may be attributed to the radiation-induced generation of electron hopping sites and the formation of extended pi-bonded chemical structures which are not present in the pristine material. After AO-exposure, the bulk resistivity of

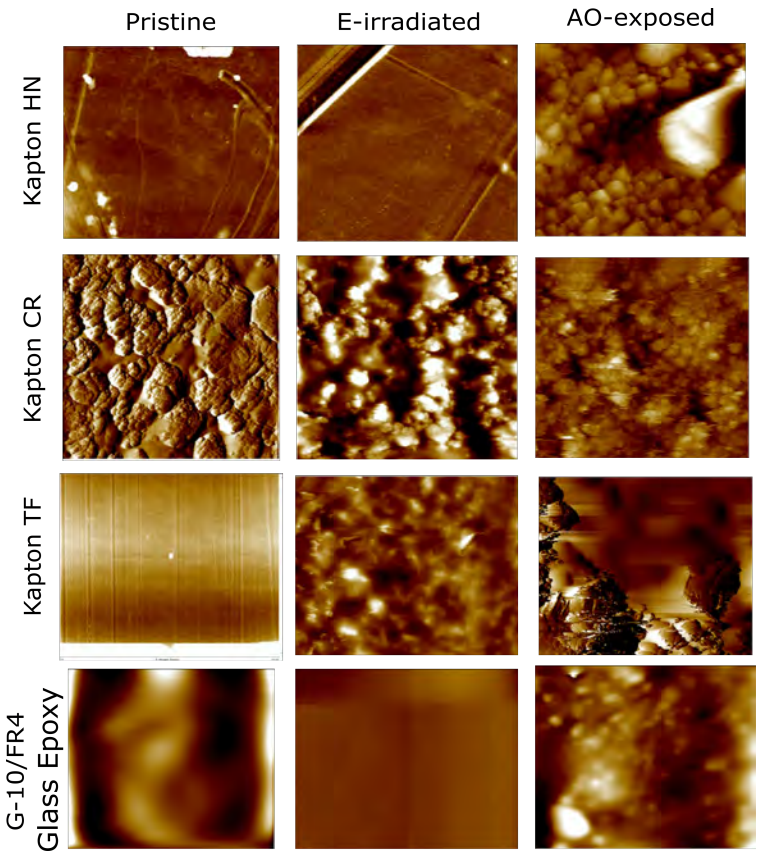

Fig. 3 Representative 5μm x 5μm AFM scans of pristine, electron-irradiated, and AO-exposed materials. Results of VUV-exposed materials will be shown during the presentation.

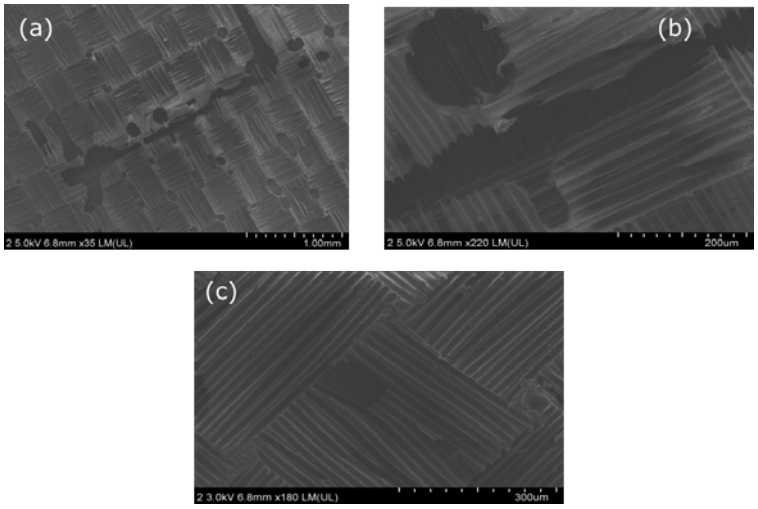

Fig. 4 (a, b) Representative SEM images of AO-exposed and (c) pristine CFRP material

the PI materials did not change significantly. The similar observation was published by Mundari et al [25], suggesting that the primary effect of AO-exposure, the roughening of the surface by the AO beam, causes an increase of surface resistivity. This roughening of the sample surface due to AO-exposure will increases the net distance that the electrons have to travel on the material surface, hence producing higher resistivity to the electron flow. Since AO-exposure affects

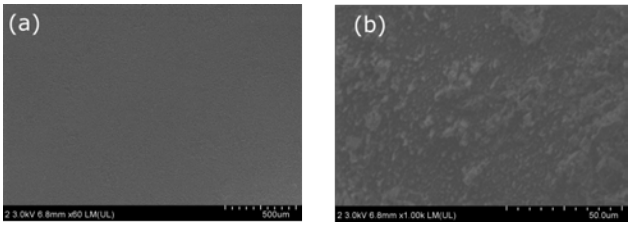

Fig. 5 Representative SEM images of AO-exposed GFRP material taken with different magnification: (a) 500 nm, (b) 50 nm.

Materials	Volume resistivity ρ x 10^{18} (Ω ṡcm)			
	Pristine		E-irradiated	
	ASTM	SPD	ASTM	SPD
Kapton® HN	5.6	8.0	0.09	0.1
Kapton® CR	13	8.6	0.008	0.8
Kapton® TF	3.6	7.9	0.07	1.0
CFRP	2.4 x 10^{-8}	0.1	1.4 x 10^{-9}	0.5
GFRP	420	0.6	0.01	2.4 x 10^{4}

Fig. 6 Resistivity of pristine and electron irradiated materials measured by ASTM and SPD methods.

Materials	Volume resistivity ρ x 10^{18} (Ω · cm) measured by ASTM	
	Pristine	AO-irradiated
Kapton® HN	2.7 × 10^{15}	3.6 × 10^{15}
Kapton® CR	5.2 × 10^{15}	6.5 × 10^{15}
Kapton® TF	1.3 × 10^{16}	3.2 × 10^{16}
CFRP	2.6 × 10^{7}	2.6 × 10^{7}
GFRP	1.2 × 10^{16}	1.2 × 10^{16}

Fig. 7 Resistivity of pristine and AO-exposed materials measured by ASTM method.

the surface morphology, not the bulk properties or bulk structure of the material, the observed no bulk resistivity change is reasonable. The same argument is applicable to the AO effect of CFRP and GFRP materials, which bulk resistivity values were also not affected by the AO exposure.

Mass loss and the relative (to Kapton®H) erosion rate were evaluated and are presented in Table 2. The erosion rates for the samples ranged from .17 to 1.70, relative to the erosion rate of the Kapton®H witness samples.

Figure 8 displays the absolute reflectance spectra of pristine and irradiated with high-energy electrons polymer materials. Irradiation with maximum electron fluence degraded the reflectance of each material from the Kapton®family in 450 - 1000 nm range. Degree of the change depends on the material, with maximum degradation demonstrated by the Kapton®TF. The GFRP material also demonstrated decrease of the signal in 400 - 600 nm range. The black materials, CFRP, did not reveal any change of optical characteristics measured by DHR.

Results of UV-Vis transmission measurements of transparent pristine and AO-exposed materials are presented in Figure 9.Light transmission characteristics of all studied materials considerably degraded after AO exposure. The measurable (e.i., transparent enough) materials from the Kapton®family (HN, TF, and CR) demonstrated reduction of transmission signal. The GFRP material have low light transmittance in its pristine state (0.1-0.2 percent), and after atomic oxygen exposure its appearance has changed to completely opaque.

Figure 10 demonstrates the results of HCRF measurements of for pristine, electron irradiated, and AO-exposed

Table 2 Mass loss and the relative (to Kapton®H) erosion rate of AO-irradiated materials.

Material	Mass loss (mg)	Erosion rate
Kapton®HN	7.76	1.57
Kapton®CR	0.84	0.18
Kapton®TF	9.16	1.19
CFRP	8.10	1.71
GFRP	4.00	1.10

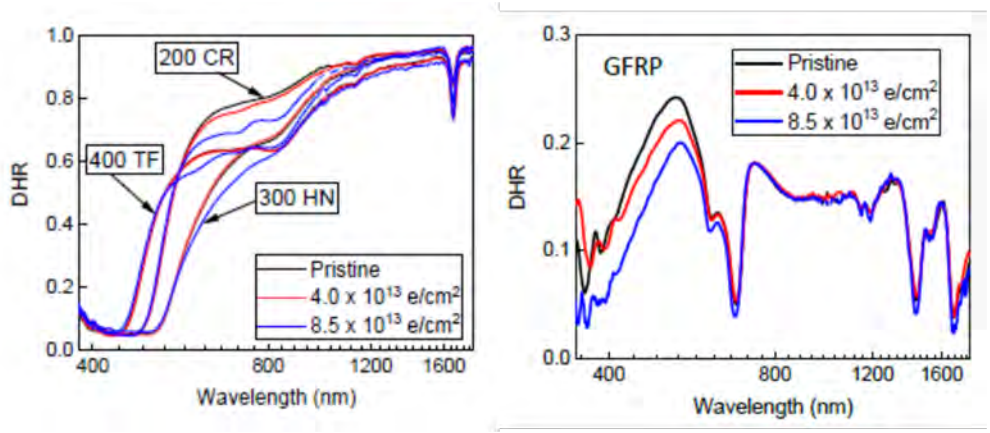

Fig. 8 DHR values of pristine and irradiated with high-energy electrons materials: (left panel) Kapton®HN, CR, and TF, (right panel) GFRP.

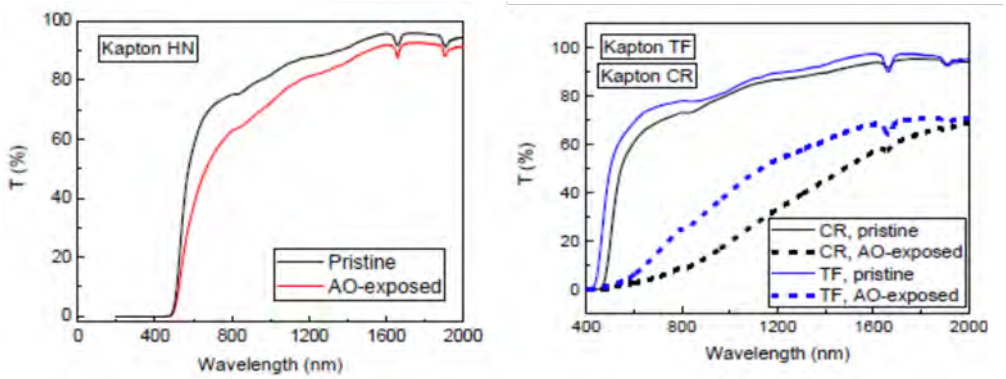

Fig. 9 UV-Vis transmission measurements of pristine and AO-exposed materials: (left panel) Kapton®HN, (right panel) Kapton®CR and TF.

materials performed at one of the fixed viewing angles (0°) and variable illumination angles. It should be noted that all studied materials showed a significant reduction in specular reflection – both in terms of the peak specular signature and the width of the specular lobe.

IV. Conclusions

Thorough physical and chemical characterization of novel and heritage spacecraft materials during the simulated space weather experiments is important for establishment of correlation factors between true space-exposure and accelerated space weather experiments at ground facilities as well as enabling accurate prediction of on-orbit material performance based on laboratory-based testing. This work focuses on characterization of material properties of selected

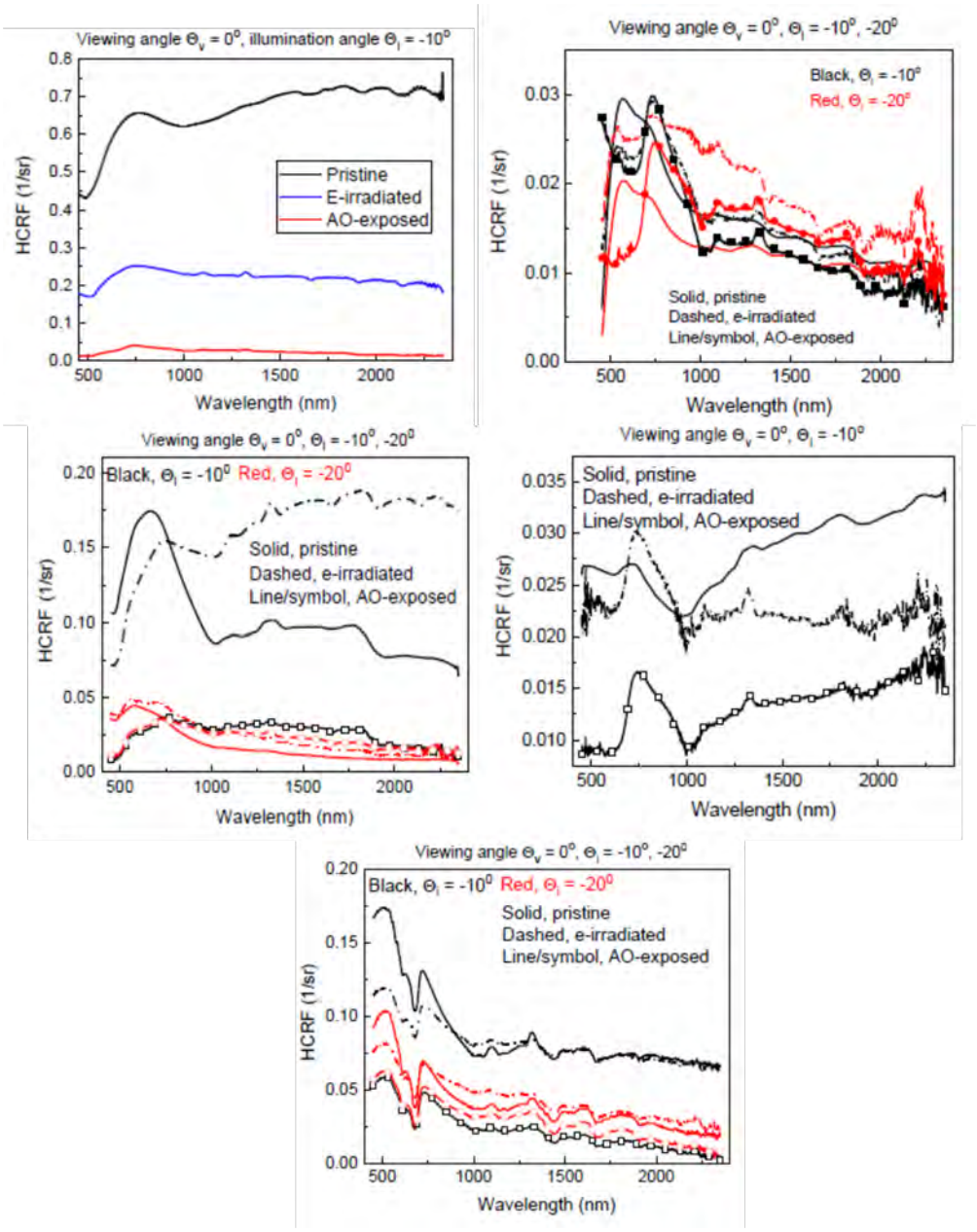

Fig. 10 HCRF measured for pristine, electron-irradiated, and AO-exposed materials measured fixed viewing angle (0°) and variable illumination angles.

spacecraft materials under independent LEO-simulated electron irradiation, AO, and VUV exposure. In addition, results of optical changes of the same materials selection under true space exposure during the 6 months LEO mission will be discussed during the presentation.

V. Acknowledgements

Authors gratefully acknowledge Physical Sciences, Inc., especially Drs. Daniel M. Hewett and David B. Oakes, for conducting AO-exposure experiments. Authors also would like to thank DuPont de Nemours, Inc, for providing polyimide materials for this research. This work was partially supported by Air Force Office of Scientific Research, Remote Sensing and Imaging Physics Portfolio (Dr. Michael Yakes) Grant 20RVCOR024 and Georgia Tech Research

Institute Independent Research and Development (IRAD) program.

Disclaimers

The views expressed are those of the author and do not necessarily reflect the official policy or position of the Department of the Air Force, the Department of Defense, or the U.S. government.

Trade names and trademarks are used in this report for identification only. Their usage does not constitute an official endorsement, either expressed or implied, by the National Aeronautics and Space Administration.

References

[1] Dooling, D., *Material selection guidelines to limit atomic oxygen effects on spacecraft surfaces*, Marshall Space Flight Center, 1999.

[2] de Groh, K. K., and Banks, B. A., "MISSE 2 PEACE polymers erosion morphology studies," *Proceedings of the International Symposium on Materials in a Space Environment (ISMSE-11)*, 2009.

[3] Miller, S. K., and Dever, J. A., "Materials international space station experiment 5 polymer film thermal control experiment," *Journal of Spacecraft and Rockets*, Vol. 48, No. 2, 2011, pp. 240–245.

[4] Ouchen, F., Aga, R., Harvey, M., and Heckman, E., "Space survivability for printed electronics applications," *Flexible and Printed Electronics*, Vol. 6, No. 1, 2021, p. 015012.

[5] Pilipenko, V., Yagova, N., Romanova, N., and Allen, J., "Statistical relationships between satellite anomalies at geostationary orbit and high-energy particles," *Advances in Space Research*, Vol. 37, No. 6, 2006, pp. 1192–1205.

[6] Lu, Y., Shao, Q., Yue, H., and Yang, F., "A review of the space environment effects on spacecraft in different orbits," *IEEE access*, Vol. 7, 2019, pp. 93473–93488.

[7] McKnight, D., Witner, R., Letizia, F., Lemmens, S., Anselmo, L., Pardini, C., Rossi, A., Kunstadter, C., Kawamoto, S., Aslanov, V., Perez, J.-C. D., Ruch, V., Lewis, H., Nicolls, M., Jing, L., Dan, S., Dongfang, W., Barranov, A., and Grishko, D., "Identifying the 50 statistically-most-concerning derelict objects in LEO," *Acta Astronautica*, Vol. 181, 2021, pp. 282–291.

[8] Reyes, J. A., and Cowardin, H. M., "Spectral characterization of spacecraft materials used in hypervelocity impact testing," *Algorithms, Technologies, and Applications for Multispectral and Hyperspectral Imaging XXVII*, Vol. 11727, International Society for Optics and Photonics, 2021, p. 117271G.

[9] Gordo, P., Frederico, T., Melício, R., Duzellier, S., and Amorim, A., "System for space materials evaluation in LEO environment," *Advances in Space Research*, Vol. 66, No. 2, 2020, pp. 307–320.

[10] Duzellier, S., Gordo, P., Melicio, R., Valério, D., Millinger, M., and Amorim, A., "Space debris generation in GEO: Space materials testing and evaluation," *Acta Astronautica*, Vol. 192, 2022, pp. 258–275.

[11] Engelhart, D. P., Plis, E., Humagain, S., Greenbaum, S., Ferguson, D., Cooper, R., and Hoffmann, R., "Chemical and electrical dynamics of polyimide film damaged by electron radiation," *IEEE Transactions on Plasma Science*, Vol. 45, No. 9, 2017, pp. 2573–2577.

[12] Kupchishin, A., Taipova, B., Lisitsyn, V. M., and Niyazov, M., "Study of the influence of the electron irradiation dose on the deformation of mylar films taking into account the processes of destruction and crosslinking," *IOP Conference Series: Materials Science and Engineering*, Vol. 510, IOP Publishing, 2019, p. 012025.

[13] Robertson, I. M., Schuh, C. A., Vetrano, J. S., Browning, N. D., Field, D. P., Jensen, D. J., Miller, M. K., Baker, I., Dunand, D. C., Dunin-Borkowski, R., et al., "Towards an integrated materials characterization toolbox," *Journal of Materials Research*, Vol. 26, No. 11, 2011, pp. 1341–1383.

[14] Cooper, R., and Hoffman, R., "Jumbo space environment simulation and spacecraft charging chamber characterization," Tech. rep., Air Force Research Laboratory, Space Vehicles Directorate Kirtland AFB . . . , 2015.

[15] Krech, R., and Caledonia, G., "Novel oxygen atom source for material degradation studies. Final report, 1 March 1986-1 September 1988," Tech. rep., Physical Sciences, Inc., Andover, MA (United States), 1988.

[16] deGroh, K. K., Dever, J. A., Jaworske, D. A., Miller, S. K., Sechkar, E. A., Panko, S. R., et al., "NASA Glenn research center's materials international space station experiments (MISSE 1-7)," 2008.

[17] de Groh, K. K., and Banks, B. A., "Atomic Oxygen Interactions and the Design of MISSE-9 and MISSE-10 Experiments," 2018.

[18] Collman, S., Plis, E., Shah, J., Hoffmann, R., and Ferguson, D., "Operational procedure for handling of spacecraft materials sensitive to atmospheric exposure," , 2022.

[19] Plis, E. A., Engelhart, D. P., Cooper, R., Johnston, W. R., Ferguson, D., and Hoffmann, R., "Review of radiation-induced effects in polyimide," *Applied Sciences*, Vol. 9, No. 10, 2019, p. 1999.

[20] Dagras, S., Eck, J., Tonon, C., and Lavielle, D., "Adhesives in space environment," *Handbook of adhesion technology. Cham: Springer*, 2018.

[21] Plis, E., Bengtson, M., Engelhart, D. P., Badura, G., Scott, T., Cowardin, H., Reyes, J., Hoffmann, R., Sokolovskiy, A., Ferguson, D. C., et al., "Characterization of novel spacecraft materials under high energy electron and atomic oxygen exposure," *AIAA SCITECH 2022 Forum*, 2022, p. 0797.

[22] Bengtson, M., Maxwell, J., Hoffmann, R., Cooper, R., Schieffer, S., Ferguson, D., Johnston, W. R., Cowardin, H., Plis, E., and Engelhart, D., "Optical characterization of commonly used thermal control paints in a simulated GEO environment," *The Advanced Maui Optical and Space Surveillance Technologies Conference*, 2018, p. 33.

[23] Badura, G., Plis, E., and Valenta, C. R., "Extending Laboratory BRDF Measurements towards Radiometric Modeling of Resident Space Object Spectral Signature Mixing," ????

[24] Frederickson, A. R., and Dennison, J., "Measurement of conductivity and charge storage in insulators related to spacecraft charging," *IEEE Transactions on Nuclear Science*, Vol. 50, No. 6, 2003, pp. 2284–2291.

[25] Mundari, N. D. A., Khan, A. R., Chiga, M., Okumura, T., Masui, H., Iwata, M., Toyoda, K., and Cho, M., "Effect of atomic oxygen exposure on surface resistivity change of spacecraft insulator material," *Transactions of the Japan Society for Aeronautical and Space Sciences, Aerospace Technology Japan*, Vol. 9, 2011, pp. 1–8.